STORM EVENT FLOW AND SEDIMENT SIMULATIONS IN A CENTRAL NEW YORK WATERSHED: MODEL TESTING AND PARAMETER ANALYSES

P. Gao, D. K. Borah, C. Yi

ABSTRACT. *In this study, we tested the prediction ability of the Dynamic Watershed Simulation Model (DWSM), an event-based watershed model, on an agricultural watershed in central New York State and its ability for use as a management tool. Using five different storm events, we identified a set of key parameters that allowed DWSM to best predict hydrographs and sedigraphs of the events for both the curve number and interception-infiltration rainfall-runoff methods. Subsequent sensitivity analyses revealed that modeling outcomes (i.e., peak water and sediment discharges, total event runoff volume, and event sediment yield) were most sensitive for the first method to CNAF, a factor adjusting runoff CN values, and most sensitive for the second method to HYCND and VOG, parameters reflecting soil hydraulic conductivity and interception loss. These analyses led to benchmark values of the key parameters and empirical relationships between precipitation and the three most sensitive parameters, which were validated using two additional storm events. Based on these results, we propose a general modeling procedure that can best predict event hydrographs and sedigraphs for watershed management planning.*

Keywords. *DWSM, Sediment transport, Watershed modeling.*

Suspended sediment transported in the stream network of a watershed not only adversely affects the hydrological, geomorphological, and ecological functioning of rivers (Owens et al., 2005) but also degrades water quality by serving as a carrier for transporting nutrients, trace metals, semi-volatile organic compounds, and pesticides (USEPA, 2000). However, the dynamic processes of suspended sediment transport within a watershed are spatially and temporally complex (Ali and De Boer, 2007; Nadal-Romero et al., 2008; Wilkinson et al., 2009). Consequently, the suspended sediment load determined at one spatial scale of a watershed is not representative of that at another scale (de Vente and Poesen, 2005; FitzHugh and Mackay, 2000; Van Dijk and Bruijnzeel, 2005). Understanding the processes of suspended sediment transport at the watershed scale thus requires considerable sediment data measured in the field at multiple spatial and temporal scales (Krishnaswamy et al., 2001; Mano et al., 2009; Smith et al., 2011), which unfortunately is often not available in practice. Furthermore, individual flood events have caused more and more damage in recent years (Kohn et al., 2014; Lavers and Villarini, 2013; Mendizabal et al., 2014), which calls for cost-effective management tools for estimating short-term variations in flow and sediment transport at the watershed scale. The goal of this case study was thus to seek a cost-effective management tool that can estimate event-based erosion and sediment transport in a typical agricultural watershed in central New York State.

An obvious cost-effective tool for managing short-term sediment dynamics relies on watershed modeling. Nonetheless, a large number of the watershed models developed thus far (Gao, 2008; Singh and Frevert, 2006) make model selection a challenging task. The most appropriate model should be physically based and have a relatively simple spatial structure. Although a variety of physically based models are available (Borah and Bera, 2003, 2004), we selected DWSM (Dynamic Watershed Simulation Model) in this study because of its (1) relatively high modeling efficiency (Borah, 2011), (2) relatively simple model structure (Borah et al., 2002), and (3) ability to capture event-based sediment dynamics (Borah et al., 2004; Borah and Bera, 2004).

DWSM is a physically based model that uses a set of governing equations to describe hydrological processes, including rainfall excess, flow routing, subsurface flow, and sediment entrainment and transport, both on hillslopes and in stream channels during one rainfall event (Borah et al., 2002, 2004). Spatially, DWSM divides a watershed into overland elements and connected stream segments, forming a network that allows water and sediment discharges derived from all overland elements and streams to be transported to the watershed outlet. DWSM has been successfully calibrated and validated in Georgia, Illinois, and Missis-

Submitted for review in October 2014 as manuscript number NRES 11018; approved for publication by the Natural Resources & Environmental Systems Community of ASABE in July 2015.

The authors are **Peng Gao,** Associate Professor, Department of Geography, Syracuse University, Syracuse, New York; **Deva K. Borah,** President, Borah Hydro-Environmental Modeling, LLC, Chesapeake, Virginia; **Chang Yi,** Research Scientist, Department of Geography, Syracuse University, Syracuse, New York. **Corresponding author:** Peng Gao, 144 Eggers Hall, Syracuse University, Syracuse, NY 13244; phone: 315-443-3679; e-mail: pegao@maxwell.syr.edu.

sippi for watersheds that have significantly diverse sizes and physiographic conditions (Borah, et al., 2007; Borah et al., 2002) and applied to both artificial and natural watersheds in China (Van Liew, 1998; Zhang et al., 2012; Zheng et al., 2008). In our preliminary study (Gao et al., 2013), we showed that DWSM can also successfully characterize event-based hydrological and sediment transport processes in an agricultural watershed in central New York State, which is our current study watershed.

However, our preliminary study only tested DWSM for two large rainfall events, which is insufficient to guarantee its predictability for small events because rainfall-runoff processes in small events are difficult to capture. An even more important issue that was beyond the scope of the preliminary study concerns whether the validated parameters for large events may lead to good predictions for small events. Additionally, the preliminary study was incapable of addressing how model parameters change over a group of events and whether DWSM may be used as a robust management tool.

Therefore, the objectives of this study are to (1) test DWSM in the study watershed using observed data from seven storm events with variable intensities and durations, and (2) provide a general procedure for using DWSM with specific values of key parameters to estimate event-based water and sediment discharges for watershed management planning. We accomplished the first objective by testing the two different rainfall-runoff methods adopted in DWSM for describing rainfall excess processes, examining the variability of adjustable parameters among five storm events, and performing sensitivity analyses for the adjustable parameters to reveal the impact of the associated hydrological and erosion processes on the predicted hydrographs and sedigraphs. We achieved the second objective by developing benchmark values for the key parameters, verifying their usage with two additional storm events, and providing a general procedure for modeling event-based hydrological and sediment transport processes in the study watershed.

Study Area and Model Structure

Oneida Creek watershed is one of the seven watersheds discharging to Oneida Lake in central New York State. It has a typical continental climate with moderate temperatures and rainfalls in summer and cold, intensive snowfalls in winter. The mean annual precipitation is more than 1270 mm. Topographically, the downstream part of the watershed is quite flat, while the middle and upstream parts vary in elevation from 120 to 570 m. The study area is the middle and upper sections of the Oneida Creek watershed with an area of 311 km^2 and thus is a medium-sized watershed (Singh, 1995). The main land use and land cover types are crop lands (23%), pasture (17%), forest (23%), urban (20%), and wetland/open water (7%), with agricultural and urban lands dispersed throughout the entire watershed (fig. 1). The Oneida Creek watershed supplies significantly higher sediment loads than other watersheds draining to Oneida Lake and serves as the main source of sediment pollution to the lake. The variability in soils in the watershed is a function of the topography and parent material. Approximately 64% of the soils in the watershed developed from glacial till. The till is generally high in calcareous material, and soil textures are loam and silt loam. Soils closer to the lake, which belongs to the Erie Ontario Lake Plain, formed in glaciofluvial parent material (23% of the watershed). The texture of this material is largely a function of the speed of receding glacial melt water and ranges from sands and gravels deposited by rapidly flowing water to silts and clays that accumulated as water evaporated from glacial lakes. Organic soils comprise approximately 3% of the soils in the watershed. The dominant soil hydrological group is group B (fig. 1).

For DWSM modeling, the study watershed was divided into 42 overland elements (numbers 1 to 42) and 21 stream segments (numbers 43 to 63) (fig. 1) using the ArcHydro technique (Maidment, 2002). This spatial structure was generated based on DEM data of 10 m resolution and a rectified stream network shapefile. The delineated overland elements range in size from 1.13 to 16.12 km^2. This spatial arrangement ensures that each overland element is not so small that the connection structure among elements is overcomplicated.

Methods

Rainfall Information

Although we measured precipitation using a tipping-bucket rain gauge installed at the outlet of the study watershed, these data were not usable because of malfunction of the equipment and unexpected bird disturbances. Instead, we used hourly precipitation data recorded at the nearest NOAA weather site (Rome, N.Y.). Additionally, we obtained daily cumulative precipitation at three sites around the study watershed from the Community Collaborative Rain, Hail, and Snow (CoCoRaHS) network (www.cocorahs.org) to verify the NOAA data. Based on annual precipitation records and the associated peak discharges, we divided the selected storm events into (relatively) large and small events in terms of a threshold value of 40 mm.

Determination of Water and Sediment Discharges during Storm Events

Stages were recorded and water samples were collected at a monitoring station established at the outlet of the study watershed (fig. 1). The monitoring station used an ISCO automatic pumping sampler for obtaining sediment concentrations (*C*). Water discharges (*Q*) of storm events were determined from measured stages and a regression between measured *Q* at the outlet and the associated *Q* recorded at a USGS gauging station located slightly upstream. Sediment discharge (Q_s) was determined using the established Q_s-Q relationship. The medium size of sediment fraction (D_{50}), determined by averaging the results obtained from particle size analysis of three samples collected from three different events, was between 0.014 and 0.02 mm. More details are provided by Gao and Josefson (2012). The total runoff volume and sediment load for each event were calculated based on the storm flow of the event.

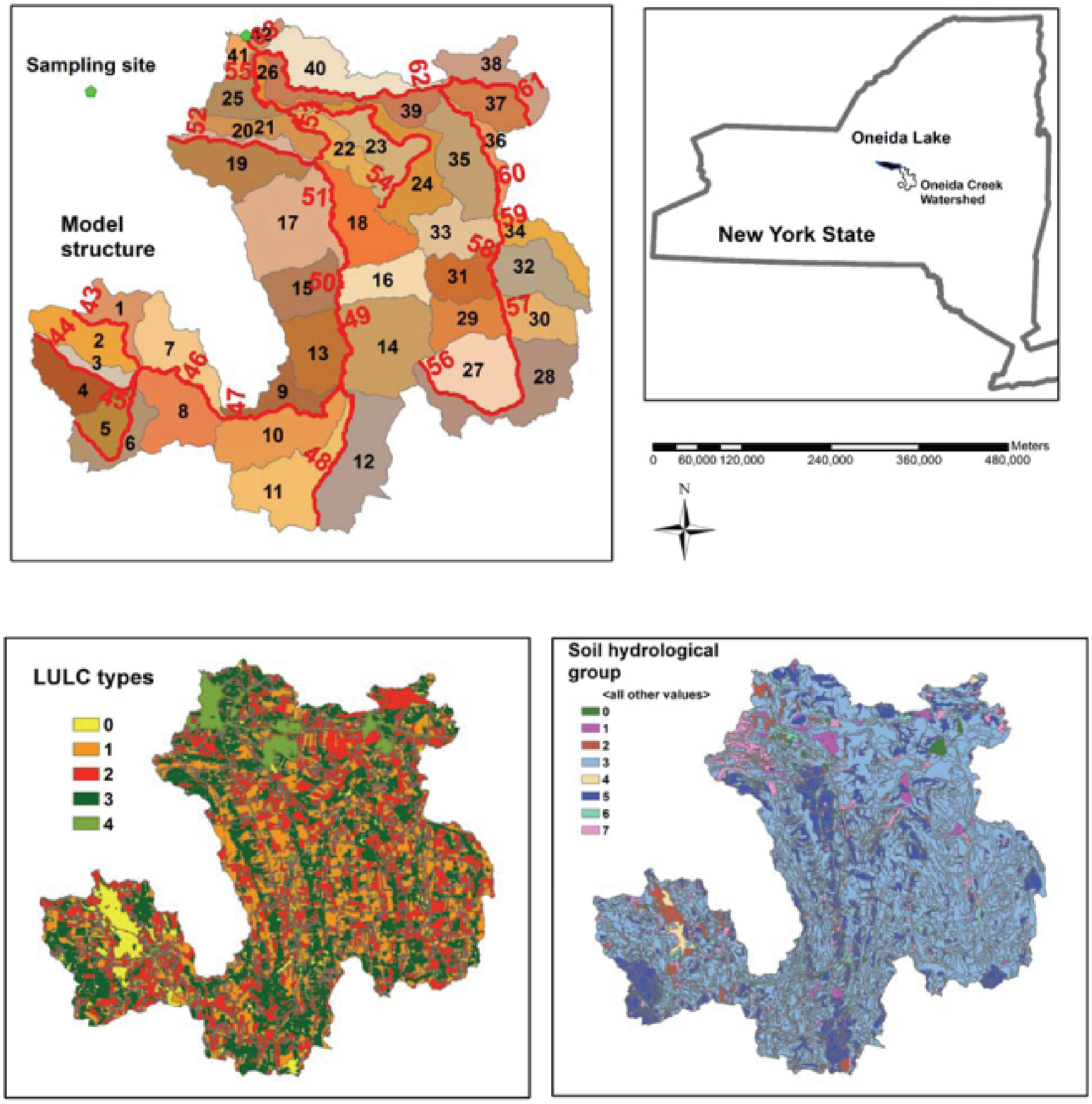

Figure 1. Study watershed (upper right), model structure (upper left), distribution of soil hydraulic groups (lower right), and land use and land cover (lower left). Land use and land cover (LULC) types: 0 = wetland/open water, 1 = crop lands, 2 = pasture, 3 = forest, and 4 = urban lands. Soil hydrological groups: 0 = no value, 1 = group A, 2 = group A/D, 3 = group B, 4 = group B/D, 5 = group C, 6 = group C/D, 7 = group D.

DWSM Input Data Preparation

Various input parameters representing watershed morphological structure, topography, vegetation, soil, rainfall, and sediment need to be determined before simulation. These parameters can be conveniently divided into two categories: lumped and distributed parameters (table 1). Lumped parameters are single values for the entire watershed, while distributed parameters have different values for different overland elements and stream segments. CNAF, FAFO, and FAFC (table 1) are three key lumped and adjustable parameters whose changes affect at the same rate the values of curve number (CN) and friction factor (i.e., Manning's "n") for each overland element and stream segment. HLR, VIN, VOG, VOR, SRG, and EVP (table 1) are lumped vegetation parameters. Our preliminary study (Gao et al., 2013) showed that VOG is the most sensitive parameter among the five and hence is treated as an adjustable parameter. The initial values of these five parameters were adopted from those used in Illinois watersheds (Borah et al., 2004). The value of the lumped rainfall parameter (GMAX) used in earlier applications by Borah et al. (2002) was adopted here. TEMP was assigned as 20°C in this study. The values of GAMA and SNU were the same as those used by Borah et al. (2002). RDC does not have a significant impact on modeling results, and hence its value was kept at 1.0 as in our preliminary study (Gao et al., 2013; Borah et al., 2002).

Table 1. Main model input parameters.

Input Parameters		Definition	Type
Main adjustable	CNAF	Uniform CN adjustment factor	Lumped
	FAFO	Uniform friction adjustment factor for overland elements	Lumped
	FAFC	Uniform friction adjustment factor for stream segments	Lumped
Topography	OVA	Overland area (acres)	Distributed
	SLEN	Slope length (ft)	Distributed
	SLOPE	Average slope (%)	Distributed
	FRICO	Manning's "n" for overland elements	Distributed
	FRICC	Manning's "n" for stream segments	Distributed
	CN	Runoff curve number	Distributed
	CPER	Coefficient of wetted perimeter and flow area relationship	Distributed
	EPER	Exponent of wetted perimeter and flow area relationship	Distributed
Vegetation	CANO	Canopy cover density for overland elements	Distributed
	GCOV	Ground cover density for overland elements	Distributed
	HLR	Average height of ground cover in stream segments (ft)	Lumped
	VIN	Initial interception storage	Lumped
	VOG	Interception storage capacity of ground cover (in.)	Lumped
	VOR	Ratio of interception storage capacity of canopy cover to that of ground cover	Lumped
	SRG	Ratio of evaporation surface to projected area of ground cover	Lumped
	EVP	Mean evaporation rate (in. h^{-1})	Lumped
Soil	COND	Effective lateral saturated hydraulic conductivity (in. h^{-1})	Distributed
	CONT	Initial uniform moisture content in the soil/porous zone	Distributed
	HYCND	Vertical soil hydraulic conductivity for overland elements (in. h^{-1})	Distributed
	SORPTY	Soil sorptivity for overland elements (in. h^{-1})	Distributed
Rainfall	GMAX	Maximum raindrop penetration depth (ft)	Lumped
	TEMP	Water temperature (°C)	Lumped
Sediment	RDC	Rainfall detachment coefficient	Lumped
	FDCI	Flow detachment coefficient	Distributed
	PC	Percentage of sediment fraction	Lumped
	D_{50}	Median size of sediment fraction (mm)	Lumped
	GAMA	Specific weight of water (lb ft^{-3})	Lumped
	SNU	Kinematic viscosity of water ($\times 10^5$ ft^2 s^{-1})	Lumped

The distributed topographic parameters (OVA, SLEN, and SLOPE) for overland elements and stream segments were determined using 10 m DEM data and stream network data in ArcGIS. Manning's "n" for each overland element and stream segment (i.e., FRICO and FRICC in table 1) was determined following a commonly used guide (Arcement and Schneider, 1984) and the observations of our field survey. Runoff curve numbers for all overland elements (i.e., CN in table 1) were determined using GIS techniques based on the land use and land cover (LULC) and soil maps shown in figure 1. Values of CPER and EPER for stream segments were determined using our survey data at multiple channel sections and the reference reach spreadsheet (v4.2 level) developed for channel survey management (Mecklenburg, 2006). CANO was assumed to be proportional to forest cover, and its values for overland elements were determined based on the area-weighted percentage of forest (fig. 1). GCOV was assumed to be proportional to impervious surface, and its values for overland elements were determined based on the area-weighted percentage of urban (fig. 1). Hydrologically, CONT is related to soil precedent condition, which is affected by the time interval between two storm events. It is very hard to quantify in practice. Fortunately, the value of CONT did not have a significant impact on modeling results. Therefore, we assumed that its variation among overland elements was proportional to the area-weighted percentage of forest. The final values were subsequently adjusted to the same range as those used in our previous study. HYCND, SORPTY, and COND are three different, but relevant, distributed parameters, so we used the calculated area-weighted soil K factor (K_s) for each overland element to reflect the differences among all elements. These values served as initial values and were adjusted during model simulation. The spatially distributed values of FDCI over all elements were quantitatively represented as an inverse function of the percentages of forest and shrub because soils in elements with higher percentages of forest and shrub are more difficult to detach by flow than soils in elements with lower percentages of forest and shrub. This parameter was adjusted during simulation to achieve the best predicted sedigraphs.

TWO DIFFERENT RUNOFF SIMULATION METHODS

DWSM has two different methods for simulating rainfall excess. The first method is an extension of the SCS runoff curve number (CN) procedure (the CN method) in which the rainfall excess rate (direct runoff rate) is calculated from CN values of the overland elements and breakpoint cumulative precipitation data (Borah, 1989a):

$$Q_r = \frac{(P - 0.2S_r)^2}{P + 0.8S_r} \tag{1}$$

$$S_r = \frac{25400}{\mathrm{CN}} - 254 \tag{2}$$

$$I_{e,i} = \frac{Q_{r,i} - Q_{r,i-1}}{\Delta t_i} \tag{3}$$

where P is the accumulated rainfall (mm), i is the time step (the total number of time intervals from the beginning of simulation), Δt_i is the time interval between time steps i–1 and i (h), $I_{e,i}$ is the rainfall excess rate during time interval Δt_i (mm h^{-1}), and $Q_{r,i}$ is the accumulated direct runoff or rainfall excess at time step i (mm). The CN method calculates the volume of surface runoff based on the values of P and CN; it is relatively simple and has only one adjustable parameter (CNAF), whose change accounts for variations in the antecedent moisture conditions and estimation errors in P and CN.

The second method, the interception-infiltration method, is a procedure in which the rate of rainfall excess is calculated by subtracting rainfall losses to interception (by both tree canopies and ground cover) and infiltration from rainfall intensity (Borah et al., 2002):

$$I_e = I - D_c I_c - D_g I_g - f \quad (4)$$

where I_e is the rate of rainfall excess, I is the rainfall intensity, D_c is the canopy cover density, I_c is the rate of canopy interception, D_g is the ground cover density, I_g is the rate of ground cover interception, and f is the rate of infiltration. Values of I_c and I_g are determined based on the interception storage capacities and associated evaporation rates for canopies and ground cover, whose values are predetermined in the input file. The ponding time (t_p), which is the time period during which all rainfall on the ground infiltrates into the soil, and f are determined using the 1-D diffusion equation for water under gravity (Smith and Parlange, 1978). Further descriptions of the Smith and Parlange (1978) solutions and their adoption in DWSM are provided by Borah et al. (1981), Borah et al. (2002), and Borah (2011). Values of t_p and f are dependent on soil hydraulic conductivity and sorptivity. Losses in depressional storage are indirectly accounted for in the interception as initial losses. Selecting this method means that CN and CNAF are replaced by three adjustable parameters (VOG, HYCND, and SORPTY) to simulate rainfall-runoff processes. Both methods were used in this study to test the prediction ability of DWSM.

Surface Runoff Routing

The excess rainfall over the overland elements and through the stream segments is routed using the kinematic wave approximations (Lighthill and Whitham, 1955) of the Saint-Venant or shallow water wave equations, as described by Borah (1989a) and Borah et al. (2002). The routing scheme is based on the analytical and approximate shock-fitting solutions (Borah et al., 1980) of the continuity and approximate momentum equations. The scheme is robust because of the closed-form solutions. FAFO and FAFC are the relevant adjustable parameters used in the scheme.

Subsurface Flow Routing

A portion of the infiltrated water in an overland element flows downstream as subsurface flow and ultimately discharges laterally into the contributing channel. This flow can be accelerated due to the presence of tile drains. The kinematic storage equation used in SWAT (Arnold et al., 1998) was adopted in DWSM for subsurface flow simulations, as discussed by Borah et al. (2002, 2004). The two adjustable parameters used in these calculations are COND, representing the effective lateral saturated hydraulic conductivity, and CONT, reflecting the uniform initial moisture content of each overland element, although the latter was not significantly sensitive, as indicated earlier. Conservation of subsurface water mass is maintained by continuously updating the water volume via solution of the spatially uniform and temporally varying continuity equation (Borah et al., 2004).

Erosion and Sediment Simulations

The eroded soil or sediment in the study watershed was divided into four particle size classes. The erosion, deposition, and transport of each size class were simulated individually, and total responses in the form of sediment concentration, sediment discharge, and bed elevation change were obtained through integration of the responses from all size classes. The sediment transport capacity of the flow for a size class was computed using selected formulas from the literature, as discussed by Borah (1989b) and Borah et al. (2002).

DWSM maintains a loose soil depth in each overland element and channel bed to keep track of loose soil accumulated from bed materials detached by raindrop impact and/or from deposited sediment. Sediment entrainment takes place from this loose soil layer as long as the sediment transport capacity of the flow is higher than the sediment load, or all the materials from the layer are entrained and become part of the sediment load. If the transport capacity continues to exceed the load, the flow erodes additional soil from the parent bed material, and the potential erosion is the difference between the transport capacity and the load. Actual erosion is computed simply by multiplying the potential erosion by the only adjustable parameter, the flow detachment coefficient (FDCI) (table 1), for overland elements and stream segments (Borah, 1989b; Borah et al., 2002).

If the sediment transport capacity is lower than the sediment load, the flow is in deposition mode, and the potential rate of deposition is equal to the difference between the transport capacity and the load. The actual rate of deposition is computed by taking into account particle fall velocities (Borah, 1989b; Borah et al., 2002). From the actual erosion and deposition, the change in bed elevation during a computational time interval is computed. All these processes are interrelated and must satisfy locally the conservation principle of sediment mass expressed by the sediment continuity equation. With some approximations, the continuity equation is solved by the method of characteristics, and the solution is used to keep track of erosion, deposition, sediment discharge, and bed elevation change along the unit width of an overland element or the flow section of a stream segment (Borah, 1989b; Borah et al., 2002).

Modeling the Study Watershed

The first five storm events (two large and three small) in table 2 were selected to test the performance of DWSM. These events had various precipitation amounts and durations and hence represent typical events that generate significant storm flows and suspended sediment loads over rainfall-dominated periods in the study watershed. The September 26, 2010, event was the largest event of the year, while the August 22, 2010, event produced comparable Q_{peak} and Q_{speak}. Although the October 7 and October 14,

Table 2. Properties of storm events selected for DWSM modeling.

Storm Event	Precipitation (mm)	Duration (h)	Q_{peak} ($m^3 s^{-1}$)	Q_{speak} ($kg s^{-1}$)
June 28, 2010	36.8	72	37.1	36.1
August 22, 2010	83.1	48	62.4	50.3
September 26, 2010	100.3	84	85.4	89.3
October 7, 2010	13.7	35	32.1	28.0
October 14, 2010	16.3	80	31.7	28.3
April 17, 2010	23.1	38	17.5	7.42
June 28, 2013	58.9	15	315	1322

2010, events had apparently small amounts of precipitation, they produced peak discharges (Q_{peak}) that were comparable to those of the June 28, 2010, event with larger precipitation. These three events are representative of small events in the study watershed. For each event, values of the adjustable parameters associated with each method were changed to find the best fits for the hydrographs and sedigraphs of each of the selected storm events, as parameter values vary due to changes in the physical conditions of a watershed during a year. Understanding this variation is critical for judging model performance (Borah and Ashraf, 1990) and for using the model as a management tool. The model performance for each event was quantified using the percent error, E_p (i.e., the ratio of the difference between predicted and measured variables to the measured variable in percentage), and the coefficient of efficiency, E_c (Beven, 1993):

$$E_c = \frac{\sum_{i=1}^{n}\left(A_i^p - \overline{A}^m\right)^2 - \sum_{i=1}^{n}\left(A_i^p - A^m\right)^2}{\sum_{i=1}^{n}\left(A_i^p - \overline{A}^m\right)^2} \qquad (5)$$

where A is either Q or Q_s, $\overline{A}^m$ is the mean of measured A, and A_i^p and A_i^m are the predicted and measured values of A, respectively. Values of E_p describe the event-lumped goodness-of-fit, while values of E_c characterize the degree of synchronization between measured and simulated values for one event. Zema et al. (2012) showed that the threshold value for an acceptable prediction should be $E_c = 0.36$. This threshold was adopted as a criterion for judging model performance.

To examine the variability of the best-fitted sets of parameters, we performed sensitivity analyses for these parameters in both runoff methods using the September 26, 2010, event, as we did not see significant changes in sensitivity among the five events. The parameters used for the CN method were CNAF, FAFO, FAFC, COND, CONT, and FDCI, while the parameters used for the infiltration-interception method were VOG, HYCND, SORPTY, FAFO, FAFC, COND, CONT, and FDCI. Based on these results, we then identified the most sensitive parameters for four modeling outcomes, i.e., peak water discharge (Q_{peak}), total event runoff volume (V_{tot}), peak sediment discharge (Q_{speak}), and total event sediment load (SSY_e), and subsequently found a set of parameters that led to reasonable predictions for all five storm events. We then verified the use of these values in model prediction using two additional events, a large event (June 28, 2013) and a small event (April 17, 2010), and subsequently proposed a general modeling procedure.

RESULTS AND ANALYSIS

MODEL CALIBRATION USING FIVE STORM EVENTS

Using the CN method, the values of the six adjustable parameters were changed during the simulation, which led to a set of parameters that produced the best-fitted hydrographs and sedigraphs for the first five rainfall events (table 3). For the June 28, 2010, event, predicted peak water and sediment discharges at the watershed outlet arrived at almost the same time as the measured values, with 21.6% and 25.7% underestimation in magnitudes, respectively (table 4). The predicted hydrograph and sedigraph were generally consistent with the measured ones, which indicated 11.5% underestimation for V_{tot} and 20.6% overestimation for SSY_e. The consistency between the predicted and measured variables was further confirmed by the relatively high values of E_p (table 4). Modeling outcomes for the August 22, 2010, event were good for Q_{peak}, V_{tot}, and Q_{speak} but not for SSY_e, which was caused by an overall delay of suspended sediment concentrations and confirmed by the relatively low E_c value (fig. 2 and table 4). Because the measured Q_s values were calculated using the established sediment rating curve, which was based on a limited number of measured sediment concentrations, the calculated Q_{speak} and

Table 3. Parameter values for the best-fitted model results for the first five storm events (parameters are defined in table 1).

	CN Method						Infiltration-Interception Method							
Storm Event	CNAF	FAFO	FAFC	COND	CONT	FDCI	FAFO	FAFC	VOG	COND	CONT	FDCI	HYCND	SORPTY
June 28, 2010	1.17	3.5	1.2	0.001	0.2	0.030	3.6	3.0	0.65	0.001	0.2	0.04	0.001	0.001
Aug. 22, 2010	0.84	2.5	0.8	0.001	0.2	0.033	3.5	1.0	1.00	0.001	0.2	0.025	0.004	0.001
Sept. 26, 2010	0.86	3.0	2.0	0.001	0.4	0.050	3.1	2.0	1.50	0.003	0.2	0.07	0.004	0.001
Oct. 7, 2010	1.40	3.5	1.0	0.001	0.7	0.017	0.1	2.8	0.06	0.001	0.2	5.00	0.003	0.001
Oct. 14, 2010	1.45	3.5	2.0	0.001	0.2	0.020	2.5	3.5	0.01	0.009	0.2	0.05	0.001	0.001

Table 4. Quantitative evaluation of model results for the first five storm events.[a]

	CN Method						Infiltration-Interception Method					
	V_{tot}		SSY_e		Q_{peak}	Q_{speak}	V_{tot}		SSY_e		Q_{peak}	Q_{speak}
Storm Event	E_p (%)	E_c	E_p (%)	E_c	E_p (%)	E_p (%)	E_p (%)	E_c	E_p (%)	E_c	E_p (%)	E_p (%)
June 28, 2010	-11.5	0.71	20.6	0.74	-21.6	-25.7	3.9	0.66	1.1	0.84	1.7	-29.1
Aug. 22, 2010	-20.4	0.83	39.6	0.24	-2.8	-1.6	-24.4	0.76	18.2	0.53	4.2	-1.9
Sept. 26, 2010	-21.8	0.86	3.1	0.87	4.5	9.9	-14.6	0.79	-0.0	0.88	5.9	0.2
Oct. 7, 2010	13.0	0.92	22.5	0.65	3.3	-19.7	-13.0	0.94	19.0	0.92	2.1	0.7
Oct. 14, 2010	-10.3	0.86	36.7	0.75	2.6	-33.5	-14.0	0.87	-3.2	0.78	-0.7	-46.1

[a] V_{tot} = total event runoff volume, SSY_e = total event sediment load, Q_{peak} = peak water discharge, Q_{speak} = peak sediment discharge, E_p = percent error of prediction, and E_c = coefficient of efficiency (defined in eq. 5).

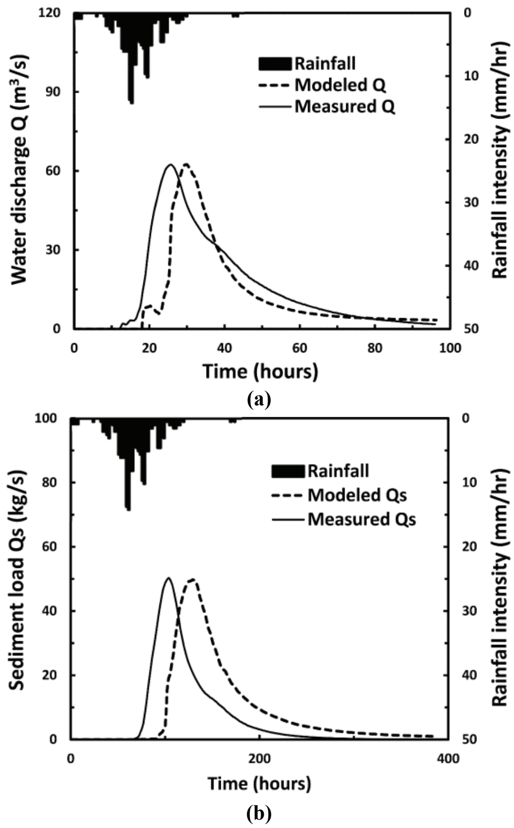

Figure 2. Example of comparing predicted and measured results for the CN method using the August 22, 2010, storm event: (a) hydrographs and (b) sedigraphs.

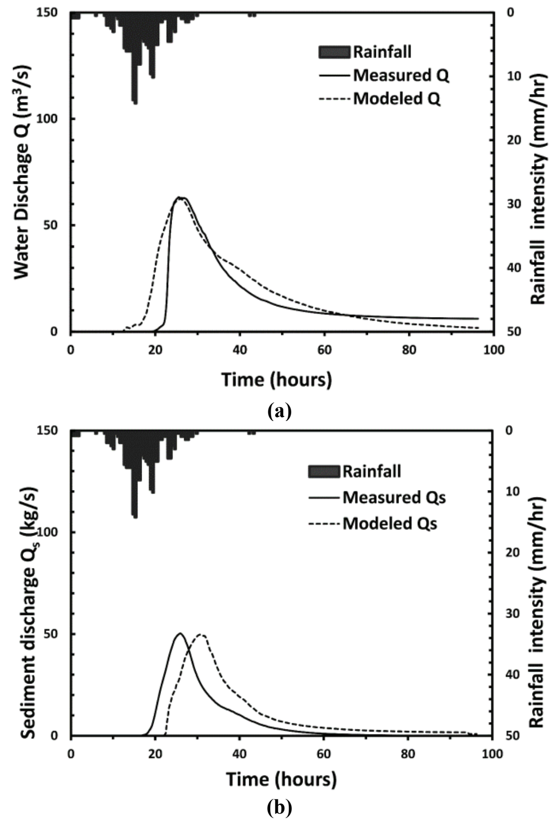

Figure 3. Example of comparing predicted and measured results for the infiltration-interception (I-I) method using the August 22, 2010, storm event: (a) hydrographs and (b) sedigraphs.

other Q_s values along the sedigraph may not be accurate, leading to the difference between the modeled and measured sedigraphs. For the largest storm event (September 26, 2010), the predicted shapes of the hydrograph and sedigraph and the four associated quantities were similar to their measured counterparts, although V_{tot} was underpredicted by 21.8% (table 4). For the two October events, the measured hydrographs were fitted better than the measured sedigraphs, which was consistent with their higher E_c values (table 4). Values of Q_{speak} were underestimated by 19.7% and 33.5%, respectively, while those of SSY_e were overestimated by 22.5% and 36.7%, respectively. Because only the E_c value for SSY_e prediction for the August 22, 2010, event was less than the threshold value, we believed that DWSM performed well for the five events. Overall, the goodness-of-fit for the five events increased as precipitation increased (tables 2 and 4). It appears that DWSM can better predict the hydrographs and sedigraphs of large storm events, which is consistent with the modeling results for other watersheds (Borah et al., 2007).

We also simulated the five events using the infiltration-interception (I-I) method. The parameters common to both methods did not necessarily have the same values (table 3). For the June 28, 2010, event, the E_p values for Q_{peak}, V_{tot}, and SSY_e were all lower than those based on the CN method, whereas the E_p value for Q_{speak} was slightly higher than that based on the CN method (table 4), indicating that predictions of hydrographs and sedigraphs based on the I-I method were generally better than those based on the CN method. The predicted shape was better for sedigraphs and about the same for hydrographs compared to those based on the CN method (table 4). For the August 22, 2010, event, the I-I method led to an improved prediction for SSY_e but slightly worse predictions for Q_{peak}, V_{tot}, and Q_{speak} (fig. 3 and table 4). The predicted shapes of the hydrograph and sedigraph were closer to those of the measured ones as compared to those created using the CN method (table 4). For the September 26, 2010, event, the predictions of Q_{peak}, V_{tot}, and SSY_e were obviously improved, while the prediction of Q_{speak} remained similar to that based on the CN method. The predicted shapes of the hydrograph and sedigraph were similar to the measured ones, akin to those based on the CN method (table 4). The predictions of Q_{speak} and SSY_e were noticeably improved (table 4). The hydrograph and sedigraph for the October 7, 2010, event as predicted by the I-I method were also closer to the measured ones with respect to those predicted by the CN method (table 4). For the October 14, 2010, event, the I-I method led to significantly improved prediction for SSY_e, while the predictions for Q_{peak}, Q_{speak}, and V_{tot} were similar to those based on the CN method (table 4). Overall, the modeling results based on the I-I method were better than those based on the CN method. However, the CN method still provided reasonable predictions for all five events despite its relative simplicity. These results indicate that DWSM is capable of characterizing event-based hydrological and sediment transport processes in the study watershed.

Model Sensitivity to Adjustable Parameters

Although the modeling results showed that DWSM is an appropriate model for reproducing the observed behavior of water movement and sediment transport during a given storm event in the study watershed, the model still cannot be applied for estimating the hydrograph and sedigraph of a future event with known precipitation because the sets of parameters used for the five selected events and two rainfall-runoff methods were different.

Sensitivity analyses (i.e., changing one parameter while holding the others constant) for the CN method indicated that changes in FAFO, FAFC, COND, and CONT had limited, but variable, effects on the predicted Q_{peak} (fig. 4a). For example, a 10% increase in FAFO and FAFC led to a less than 10% and 3% decrease in Q_{peak}, respectively. However, a less than 5% change in CNAF could easily cause a change of more than one order of magnitude in Q_{peak}, indicating the significantly higher sensitivity of the modeling results to CNAF than to the other parameters. For Q_{speak}, CNAF was also the most sensitive parameter (fig. 4b). The results of the sensitivity analyses for V_{tot} and SSY_e also showed a distinctly high impact of CNAF on the modeling results. Clearly, among all the adjustable parameters, CNAF was the most sensitive, indicating that CN was the most sensitive physically based hydrologic parameter.

For the I-I method, sensitivity analyses showed that HYCND had the most significant impact on the predicted Q_{peak} and Q_{speak}. An increase of more than two orders of magnitude in Q_{peak} and about 30% change in Q_{speak} were caused by only 10% increase in HYCND (fig. 5). Changes in VOG also significantly affected the predicted values of Q_{peak}. A 10% increase in VOG led to a 17% decrease in Q_{peak} and about 20% change in Q_{speak}. A 10% change in the other parameters caused much less change in Q_{peak} and Q_{speak}. This general pattern remained for the sensitivity analyses of V_{tot} and SSY_e. Therefore, the modeling results were significantly sensitive to two parameters (HYCND and VOG) for the I-I method.

Simulation with Calibrated Parameters

For the CN method, we identified a set of values for FAFO, FAFC, COND, CONT, and FDCI with variable CNAF values that allowed the predicted hydrographs and sedigraphs to reasonably fit those of the first five storm events (table 5). For the June 28, 2010, event, the predictive errors for Q_{peak}, Q_{speak}, V_{tot}, and SSY_e were the same as those based on the best-fitted set of parameters (tables 4 and 6). For the August 22, 2010, event, the errors for Q_{peak} and SSY_e were slightly greater than, and the errors for Q_{speak} and V_{tot} were slightly less than, those based on the best-fitted set

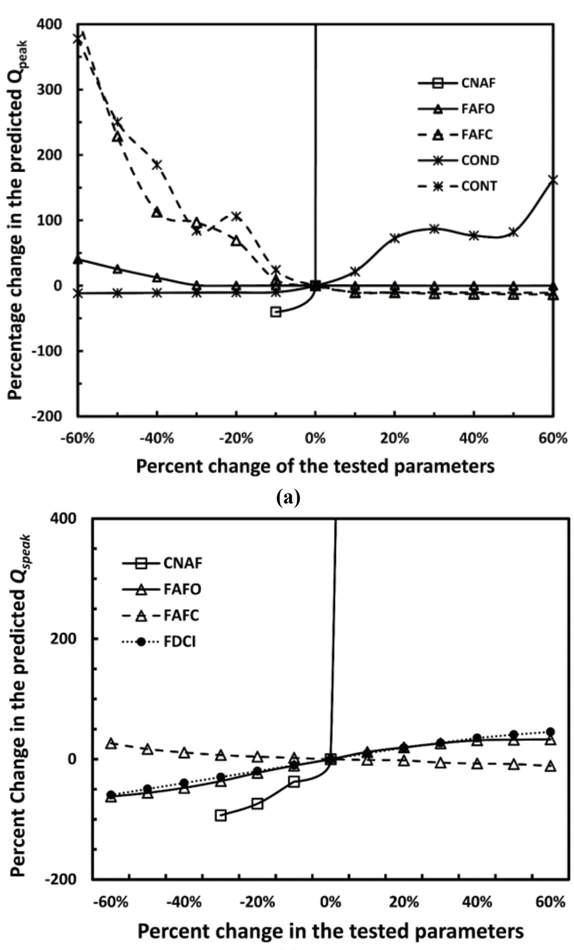

Figure 4. Example of sensitivity analysis using (a) Q_{peak} and (b) Q_{speak} for all adjustable parameters based on the CN method.

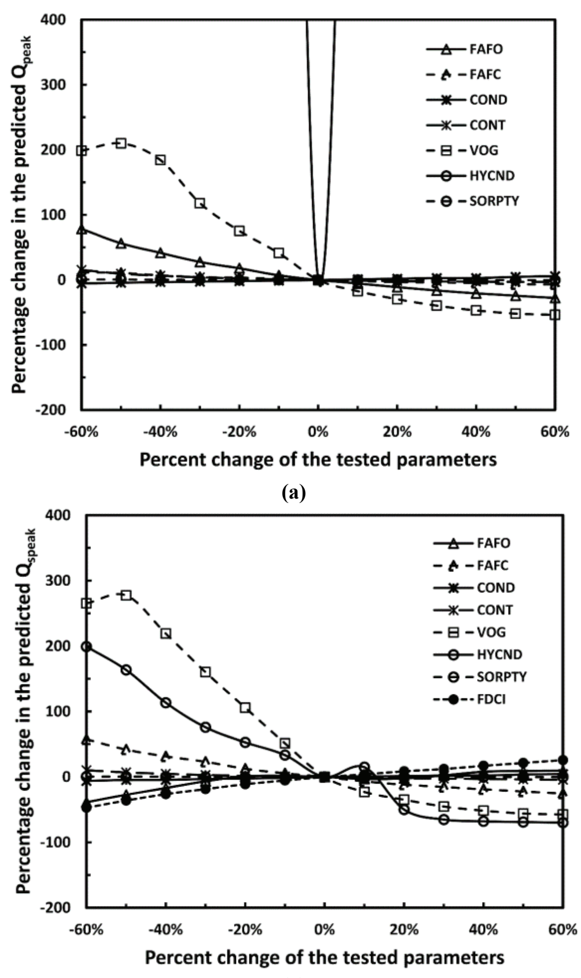

Figure 5. Example of sensitivity analysis using (a) Q_{peak} and (b) Q_{speak} for all adjustable parameters based on the I-I method.

Table 5. Parameter values with variable CNAF, VOG, and HYCND for the first five storm events (parameters are defined in table 1).

Storm Event	CN Method: CNAF	FAFO	FAFC	COND	CONT	FDCI	Infiltration-Interception Method: FAFO	FAFC	VOG	COND	CONT	FDCI	HYCND	SORPTY
June 28, 2010	1.17	3.5	1.2	0.001	0.3	0.02	3.5	1.2	0.6	0.001	0.3	0.03	0.06	0.001
Aug. 22, 2010	0.88	3.5	1.2	0.001	0.3	0.02	3.5	1.2	1.5	0.001	0.3	0.03	0.09	0.001
Sept. 26, 2010	0.85	3.5	1.2	0.001	0.3	0.02	3.5	1.2	1.7	0.001	0.3	0.03	0.095	0.001
Oct. 7, 2010	1.40	3.5	1.2	0.001	0.3	0.02	3.5	1.2	0.055	0.001	0.3	0.03	0.01	0.001
Oct. 14, 2010	1.37	3.5	1.2	0.001	0.3	0.02	3.5	1.2	0.014	0.001	0.3	0.03	0.01	0.001

Table 6. Quantitative evaluation of model results for the first five storm events with variable CNAF, VOG, and HYCND.

	CN Method						Infiltration-Interception Method					
	V_{tot}		SSY_e		Q_{peak}	Q_{speak}	V_{tot}		SSY_e		Q_{peak}	Q_{speak}
Storm Event	E_p (%)	E_c	E_p (%)	E_c	E_p (%)	E_p (%)	E_p (%)	E_c	E_p (%)	E_c	E_p (%)	E_p (%)
June 28, 2010	-11.5	0.71	20.6	0.74	-21.6	-25.7	-14.3	0.20	18.2	0.35	-8.7	-11.6
Aug. 22, 2010	-14.0	0.51	46.2	-0.15	7.4	1.3	-25.1	0.73	33.9	0.51	-6.0	20.1
Sept. 26, 2010	-2.0	0.68	-1.9	0.94	17.4	3.0	-25.8	0.8	-11.9	0.93	10.0	-1.2
Oct. 7, 2010	10.8	0.84	27.3	0.54	0.2	-11.4	-22.4	0.65	1.1	0.34	-34.1	-41.2
Oct. 14, 2010	-26.0	0.83	28.1	0.71	-31.4	-44.3	-41.3	0.78	31.4	0.60	-37.4	-38.5

of parameters. For the September 26, 2010, event, the E_p value for Q_{peak} was greater than that based on the best-fitted set of parameters, while errors for the other three variables were discernibly less than those based on the best-fitted set of parameters. For the October 7, 2010, event, only SSY_e had slightly greater error compared to that based on the best-fitted set of parameters. By contrast, for the October 14, 2010, event, only SSY_e had less error than that based on the best-fitted set of parameters. Among the first five events, only the October 14, 2010, event demonstrated overall worse performance regarding the predictive errors for Q_{peak}, Q_{speak}, V_{tot}, and SSY_e, suggesting that the identified set of parameters may generate less accurate results for relatively small storm events. However, even such less-accurate predictions are still acceptable because (1) the errors were limited (less than 45%), (2) event-based hydrological and sediment transport processes are dynamic and difficult to capture with high accuracy, and (3) the contributions of surface runoff and sediment load from small events to seasonal and annual amounts are relatively small. Therefore, the same set of the parameters may be generally applied to relatively larger storm events in the study watershed.

The variation of CNAF values among the first five events is not surprising because an earlier study showed that CNAF varied significantly among events in a year (Borah and Ashraf, 1990). However, our analysis showed that a

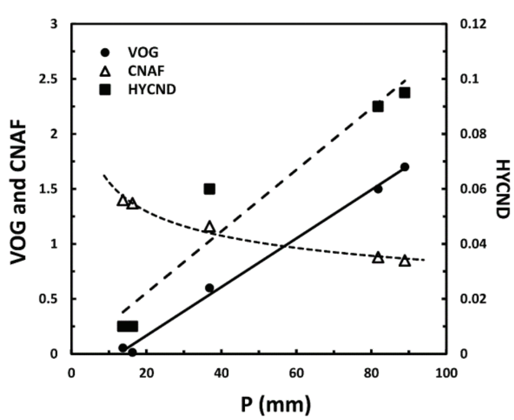

Figure 6. Empirical relationships between precipitation and the most sensitive parameters.

strong correlation existed between CNAF and the associated event precipitation (fig. 6):

$$\text{CNAF} = 2.90P^{-0.27},\ r^2 = 0.983 \quad (6)$$

where P is the precipitation of the simulated storm event. Equation 6 indicates that CNAF decreases as precipitation increases. This is at odds with the hydrological principle: a higher magnitude of precipitation tends to produce more surface runoff, which implies a higher CNAF. This apparent contradiction lies in the fact that CNAF not only reflects the antecedent soil moisture condition but also accounts for errors in the input rainfall data. Given that our modeling was based on rainfall data from only one station, the spatial distribution of a rainfall event was not accurately reflected by the input rainfall data. Therefore, the decreasing trend for CNAF with the increase in precipitation mainly reflects the adjustment of CNAF to the errors in the input rainfall data. Comparison of the CNAF values estimated using equation 6 with the predicted values for the first five events (table 5) demonstrated that the percentage errors were generally less than 2.2%, with 5.6% for June 28, 2010, and 9% for October 14, 2010, suggesting that equation 6 may provide a benchmark value for CNAF. CNAF may be further adjusted in terms of other information (e.g., a known event hydrograph) to achieve the best model prediction.

Because sensitivity analyses showed that the modeling outcomes were most sensitive to HYCND and VOG for the I-I method, we ran DWSM for the first five events with various combinations of the adjustable parameters and found a set of parameters with variable VOG and HYCND values for the five events (table 5). The prediction errors of these events were generally higher than those based on the best-fitted parameters but were still acceptable (tables 4 and 6). Although VOG and HYCND were both variable among the five events, they were highly correlated to precipitation (fig. 6):

$$\text{VOG} = 0.022P - 0.275,\ r^2 = 0.996 \quad (7a)$$

$$\text{HYCND} = 0.0011P - 0.0001,\ r^2 = 0.932 \quad (7b)$$

For the two large events (August 22, 2010, and September 26, 2010), the percentage errors between the values estimated using equations 7a and 7b and the predicted values (table 5) were less than 2% and 3% for VOG and

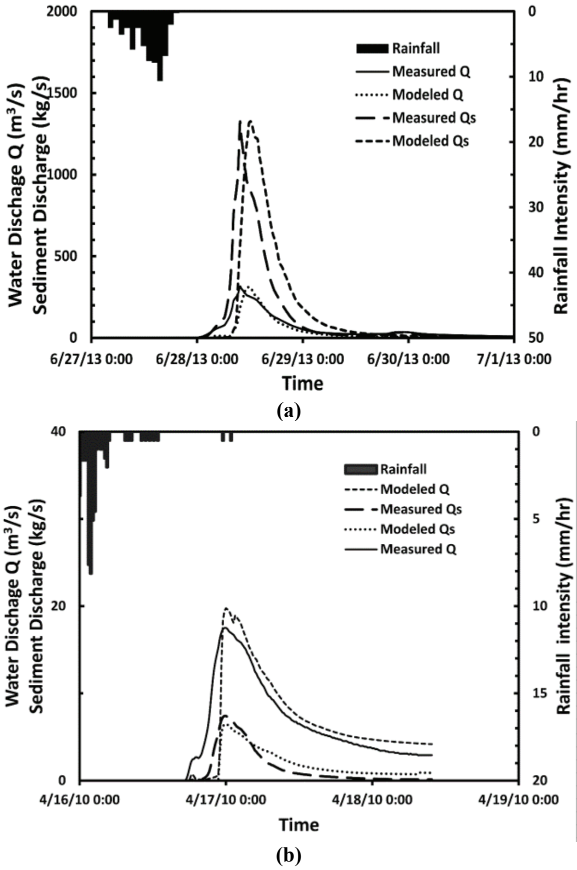

Figure 7. Example of model results for two additional events: (a) June 28, 2013, with the CN method and (b) April 17, 2010, with the infiltration-interception method.

HYCND, respectively. Again, these two equations primarily reflect the adjustment of VOG and HYCND to the errors in the input rainfall data. Therefore, for a future event, the VOG and HYCND values estimated using equations 7a and 7b can be used as benchmark values with the other identified parameters (table 5) to produce initial predictions of the hydrograph and sedigraph. The best-fitted values need to be further determined with additional information.

VALIDATION USING TWO ADDITIONAL EVENTS

Modeling the two additional events (i.e., the last two events in table 2) by changing the adjustable parameters based on table 5 and equations 6, 7a, and 7b showed that the predicted hydrographs and sedigraphs fit the measured ones well (fig. 7). Prediction errors for Q_{peak} and Q_{speak} were less than 10% for June 26, 2013, and 30% for the April 17, 2010. Predictions of V_{tot} and SSY_e using the CN method were generally better than those of the I-I method for the first event, while the inverse held for the second event (table 7). These results show that starting with the parameter values shown in table 5 and suggested by equations 6, 7a, and 7b, we may efficiently find a set of adjustable parameters that lead to acceptable predictions for the hydrograph and sedigraph of a given event in the study watershed.

DISCUSSION

PITFALLS OF DETERMINING MODEL PARAMETERS

With the same model structure (fig. 1), we were able to identify two different sets of adjustable parameters (i.e., tables 3 and 5) for both the CN and I-I methods that are acceptable for characterizing the observed hydrological and sediment transport processes for the first five storm events, suggesting the existence of uncertainties in determining these parameters. To reduce the uncertainties, we determined the initial values of the adjustable parameters based on their physical meaning and based on the literature from values used in other watersheds.

For instance, we know that the friction factors of overland elements should be greater than those of stream segments. Therefore, we ensured that changes in the associated adjustable parameters did not violate this hydraulic characteristic. In another example, the effective lateral saturated hydraulic conductivity (COND) is difficult to accurately determine *a priori*. A previous modeling study in the Court Creek watershed in Illinois (Borah et al., 2004) showed that COND = 0.01 in. h^{-1}. Compared with the Court Creek watershed, where subsurface (or lateral) flow is controlled by agricultural tile flow, lateral flow in the study watershed is dominated by soil texture and ground cover type, and hence the associated COND should be significantly less than in the Court Creek watershed. Based on this hydrological factor, values of COND for the first five events were less than 0.01 in. h^{-1} (tables 3 and 5). Following the same principle, we believe that the value of FDCI in the best-fitted set of parameters for the October 7, 2010, event (table 3) is not reasonable, although it led to relatively small predictive errors (E_p = 18.96% for SSY_e and 0.69% for Q_{speak}) (table 4). The reason is that this value is more than one order of magnitude larger than those for the other four events. Within the same season, the nature of sediment transport in the same watershed should not change dramatically from event to event, and FDCI should be constant.

APPROPRIATE USE OF THE TWO METHODS

The model calibration and validation (i.e., tables 4 and 7) both suggest that either the CN or I-I method may be used for prediction for large events, whereas the I-I method should be used for small events. Because the CN method is simpler than the I-I method, it should be used for large events. Two reasons may explain this result. First, large events are normally caused by large storms, which tend to be more uniformly distributed over the entire watershed.

Table 7. Model validation results using two additional storm events.

	CN Method				Infiltration-Interception Method			
	V_{tot}		SSY_e		V_{tot}		SSY_e	
Storm Event	E_p (%)	E_c	E_p (%)	E_c	E_p (%)	E_c	E_p (%)	E_c
June 28, 2013	34.1	0.73	18.9	0.52	-38.3	0.61	12.0	0.42
April 14, 2010	-0.52	0.64	41.2	0.31	2.47	0.60	21.2	0.73

Thus, the rainfall data series used in the input data file may represent the rainfall distribution more accurately. Second, the I-I method allows better prediction of infiltration capacity (i.e., f in eq. 4) by adjusting HYCND and SORPTY. For large events, rainfall intensity (I) is higher than infiltration capacity (f). Therefore, the rainfall excess (I_e) in equation 4 is mainly controlled by I, and more accurate prediction of f may not necessarily increase the accuracy of the prediction for I_e. For small events, however, the values of f and I are comparable, and thus better prediction of f could lead to better prediction of I_e.

Procedure for Using DWSM to Estimate Event-Based Discharges

A general modeling procedure for using DWSM to estimate the water (Q) and sediment (Q_s) discharges of a storm event or to predict those of a future event is as follows:

1. Based on the recorded or predicted precipitation, determine which method to use, i.e., the I-I method for small events or the CN method for large events.
2. For small events, values of the key parameters (i.e., FAFC, FAFO, COND, CONT, SORPTY, and FDCI) in table 5 can be adopted, and VOG and HYCND can be determined using equations 7a and 7b. Fine-tune these values in terms of the Q and Q_s of a previous similar event and predict the hydrograph and sedigraph for the target events.
3. For large events, values of the key parameters (i.e., FAFC, FAFO, COND, CONT, and FDCI) in table 5 can be adopted, and CNAF can be determined using equation 6. Using the values of Q and Q_s of a previous similar event as a reference, adjust these parameters (starting with CNAF, the most sensitive parameter) to achieve the best model prediction.

Summary and Conclusions

The Dynamic Watershed Simulation Model (DWSM), a physically based watershed model, was employed to predict the water and sediment discharges of five storm events with variable intensities and sizes in the upper Oneida Creek watershed, a medium-sized watershed in central New York State. Both the CN and infiltration-interception rainfall-runoff methods were used in these predictions, which involved six and eight adjustable parameters, respectively. For each method, we successfully identified a set of adjustable parameters that allowed DWSM to predict the measured hydrographs and sedigraphs of the five events with limited errors. These successful predictions showed that DWSM was generally capable of capturing the event-based dynamic processes of water movement and sediment transport in the study watershed. We identified the most sensitive parameters using sensitivity analysis for both methods, and we then applied the same set of less-sensitive adjustable parameters and statistical equations for the most sensitive parameters: CNAF, HYCND, and VOG, with the first expressed non-linearly (eq. 6) and the other two expressed linearly (eqs. 7b and 7a, respectively) in terms of event precipitation. These results led to a general procedure for using DWSM as a management tool to estimate event-based sediment dynamics in the study watershed, which was verified using two additional storm events. The procedure may be easily extended to other watersheds in central New York State.

The CN method is easy to perform and may be used for prediction for large storm events because of the relatively uniform distribution of rainfall and the higher rainfall intensity than infiltration capacity. The I-I method has more adjustable parameters and is more flexible. It should be used for predicting small storm events due to the more important role of infiltration capacity in determining the amount of rainfall excess. For any watershed, physical conditions vary from event to event. Therefore, it is essentially impossible to find a unique set of adjustable parameters for either of the rainfall-runoff methods that lead to accurate predictions for all events. The proposed procedure provides an efficient means of identifying the most appropriate values of the key parameters for the best model prediction. This procedure is robust and may be used as a cost-effective tool in watershed management.

Acknowledgement

The first author was partially supported by an NSF-China Grant (No. 51179016).

References

Ali, K. F., & De Boer, D. H. (2007). Spatial patterns and variation of suspended sediment yield in the upper Indus River basin, northern Pakistan. *J. Hydrol., 334*(3-4), 368-387. http://dx.doi.org/10.1016/j.jhydrol.2006.10.013.

Arcement, G. J. J., & Schneider, V. R. (1984). Guide for selecting Manning's roughness coefficients for natural channels and flood plains. USGS Water-Supply Paper 2339. Reston, Va.: U.S. Geological Survey.

Arnold, J. G., Srinivasan, R., Muttiah, R. S., & Williams, J. R. (1998). Large-area hydrological modeling and assessment: Part I. Model development. *JAWRA 34*(1), 73-89. http://dx.doi.org/10.1111/j.1752-1688.1998.tb05961.x.

Beven, K. J. (1993). Prophecy, reality, and uncertainty in distributed hydrological modeling. *Adv. Water Resources, 16*(1), 41-51. http://dx.doi.org/10.1016/0309-1708(93)90028-E.

Borah, D. K. (1989a). Runoff simulation model for small watersheds. *Trans. ASAE, 32*(3), 881-886. http://dx.doi.org/10.13031/2013.31085.

Borah, D. K. (1989b). Sediment discharge model for small watersheds. *Trans. ASAE, 32*(3), 874-880. http://dx.doi.org/10.13031/2013.31084.

Borah, D. K. (2011). Hydrologic procedures of storm event watershed models: A comprehensive review and comparison. *Hydrol. Proc., 25*(22), 3472-3489. http://dx.doi.org/10.1002/hyp.8075.

Borah, D. K., & Ashraf, M. S. (1990). Modeling storm runoff and sediment with seasonal variations. *Trans. ASAE, 33*(1), 105-110. http://dx.doi.org/10.13031/2013.31302.

Borah, D. K., & Bera, M. (2003). Watershed-scale hydrologic and nonpoint-source pollution models: Review of mathematical bases. *Trans. ASAE, 46*(6), 1553-1566. http://dx.doi.org/10.13031/2013.15644.

Borah, D. K., & Bera, M. (2004). Watershed-scale hydrologic and nonpoint-source pollution models: Review of applications.

Trans. ASAE, 47(3), 789-803. http://dx.doi.org/10.13031/2013.16110.

Borah, D. K., Prasad, S. N., & Alonso, C. V. (1980). Kinematic wave routing incorporating shock fitting. *Water Resources Res., 16*(3), 529-541. http://dx.doi.org/10.1029/WR016i003p00529.

Borah, D. K., Alonso, C., & Prasad, S. (1981). Stream channel stability: Appendix I. Single-event numerical model for routing water and sediment on small catchments. Oxford, Miss.: USDA-ARS National Sedimentation Laboratory.

Borah, D. K., Xia, R., & Bera, M. (2002). DWSM: A dynamic watershed simulation model. In V. P. Singh & D. Frevert (Eds.), *Mathematical Models of Small Watershed Hydrology and Applications* (pp. 113-166). Highlands Ranch, Colo.: Water Resources Publications.

Borah, D. K., Bera, M., & Xia, R. (2004). Storm event flow and sediment simulations in agricultural watersheds using DWSM. *Trans. ASAE, 47*(5), 1539-1559. http://dx.doi.org/10.13031/2013.17633.

Borah, D. K., Arnold, J. G., Bera, M., Krug, E. C., & Liang, X. Z. (2007). Storm event and continuous hydrologic modeling for comprehensive and efficient watershed simulations. *J. Hydrol. Eng., 12*(6), 605-616. http://dx.doi.org/10.1061/(asce)1084-0699(2007)12:6(605).

de Vente, J., & Poesen, J. (2005). Predicting soil erosion and sediment yield at the basin scale: Scale issues and semi-quantitative models. *Earth Sci. Rev., 71*(1-2), 95-125. http://dx.doi.org/10.1016/j.earscirev.2005.02.002.

FitzHugh, T. W., & Mackay, D. S. (2000). Impacts of input parameter spatial aggregation on an agricultural nonpoint-source pollution model. *J. Hydrol., 236*(1-2), 35-53. http://dx.doi.org/10.1016/S0022-1694(00)00276-6.

Gao, P. (2008). Understanding watershed suspended sediment transport. *Prog. Phys. Geography, 32*(3), 243-263. http://dx.doi.org/10.1177/0309133308094849.

Gao, P., & Josefson, M. (2012). Suspended sediment dynamics during hydrological events in a central New York watershed. *Geomorphology, 139-140*, 425-437. http://dx.doi.org/10.1016/j.geomorph.2011.11.007.

Gao, P., Borah, D. K., & Josefson, M. (2013). Evaluation of the storm event model DWSM on a medium-sized watershed in central New York. *J. Urban Environ. Eng., 7*(1), 1-7. http://dx.doi.org/10.4090/juee.2013.v7n1.001007.

Kohn, I., Rosin, K., Freudiger, D., Belz, J. U., Stahl, K., & Weiler, M. (2014). Low flow in Germany in 2011. *Hydrologie und Wasserbewirtschaftung, 58*(1), 4-17. http://dx.doi.org/10.5675/HyWa_2014,1_1.

Krishnaswamy, J., Richter, D. D., Halpin, P. N., & Hofmockel, M. S. (2001). Spatial patterns of suspended sediment yields in a humid tropical watershed in Costa Rica. *Hydrol. Proc., 15*(12), 2237-2257. http://dx.doi.org/10.1002/hyp.230.

Lavers, D. A., & Villarini, G. (2013). Were global numerical weather prediction systems capable of forecasting the extreme Colorado rainfall of 9-16 September 2013? *Geophys. Res. Letters, 40*(24), 6405-6410. http://dx.doi.org/10.1002/2013GL058282.

Lighthill, M. J., & Whitham, G. B. (1955). On kinematic waves: 1. Flood movement in long rivers. *Proc. Royal Soc. A, 229*(1178), 281-316. http://dx.doi.org/10.1098/rspa.1955.0088.

Maidment, D. R. (2002). *Arc Hydro: GIS for Water Resources*. Redlands, Cal.: ESRI.

Mano, V., Nemery, J., Belleudy, P., & Poirel, A. (2009). Assessment of suspended sediment transport in four alpine watersheds (France): Influence of the climatic regime. *Hydrol. Proc., 23*(5), 777-792. http://dx.doi.org/10.1002/hyp.7178.

Mecklenburg, D. (2006). STREAM Modules. Columbus, Ohio: Ohio Department of Natural Resources, Division of Soil and Water Conservation. Retrieved from http://soilandwater.ohiodnr.gov/water-conservation/stream-restoration#SPR.

Mendizabal, M., Sepulveda, J., & Torp, P. (2014). Climate change impacts on flood events and its consequences on human in Deba River. *Intl. J. Environ. Res., 8*(1), 221-230.

Nadal-Romero, E., Latron, J., Marti-Bono, C., & Regues, D. (2008). Temporal distribution of suspended sediment transport in a humid Mediterranean badland area: The Araguás catchment, central Pyrenees. *Geomorphology, 97*(3-4), 601-616. http://dx.doi.org/10.1016/j.geomorph.2007.09.009.

Owens, P. N., Batalla, R. J., Collins, A. J., Gomez, B., Hicks, D. M., Horowitz, A. J., Kondolf, G. M., Marden, M., Page, M. J., Peacock, D. H., Petticrew, E. L., Salomons, W., & Trustrum, N. A. (2005). Fine-grained sediment in river systems: Environmental significance and management issues. *River Res. Applic., 21*(7), 693-717. http://dx.doi.org/10.1002/rra.878.

Singh, V. P. (1995). Watershed modeling. In V. P. Singh (Ed.), *Computer Models of Watershed Hydrology* (pp. 1-22). Littleton, Colo.: Water Resources Publications.

Singh, V. P., & Frevert, D. K. (2006). *Watershed Models.* Boca Raton, Fla.: CRC Press.

Smith, R. E., & Parlange, J.-Y. (1978). A parameter-efficient hydrologic infiltration model. *Water Resources Res., 14*(3), 533-538. http://dx.doi.org/10.1029/WR014i003p00533.

Smith, S. M. C., Belmont, P., & Wilcock, P. R. (2011). Closing the gap between watershed modeling, sediment budgeting, and stream restoration. In A. Simon, S. J. Bennett, & J. M. Castro (Eds.), *Stream Restoration in Dynamic Fluvial Systems: Scientific Approaches, Analyses, and Tools* (pp. 293-317). Washington, D.C.: American Geophysical Union. http://dx.doi.org/10.1029/2011gm001085.

USEPA. (2000). The quality of our nation's waters. A summary of the National Water Quality Inventory: 1998 Report to Congress. Washington, D.C.: U.S. Environmental Protection Agency. Retrieved from http://water.epa.gov/lawsregs/guidance/cwa/305b/upload/2000_07_07_305b_98report_98brochure.pdf.

Van Dijk, A. I. J. M., & Bruijnzeel, L. A. S. (2005). Key controls and scale effects on sediment budgets: Recent findings in agricultural upland Java, Indonesia. In *Proc. Intl. Symp. on Sediment Budgets* (pp. 24-31). IAHS Publication 292. International Association of Hydrological Sciences.

Van Liew, M. W. (1998). Prediction of sediment yield on a large watershed in north central China. *Trans. ASAE, 41*(3), 599-604. http://dx.doi.org/10.13031/2013.17227.

Wilkinson, S. N., Prosser, I. P., Rustomji, P., & Read, A. M. (2009). Modelling and testing spatially distributed sediment budgets to relate erosion processes to sediment yields. *Environ. Model. Software, 24*(4), 489-501. http://dx.doi.org/10.1016/j.envsoft.2008.09.006.

Zema, D. A., Bingner, R. L., Govers, G., Licciardello, F., Denisi, P., & Zimbone, S. M. (2010). Evaluation of runoff, peak flow, and sediment yield for events simulated by the AnnAGNPS model in a Belgian agricultural watershed. *Land Degrad. Devel., 23*(3), 205-215. http://dx.doi.org/10.1002/ldr.1068.

Zhang, X. F., Zhang, X., Hu, S., Liu, T., & Li, G. H. (2012). Runoff and sediment modeling in a peri-urban artificial landscape: Case study of Olympic Forest Park in Beijing. *J. Hydrol.*, *485*, 126-138.

Zheng, Y., Fang, H., & Han, D. (2008). Principle and application of runoff yield module of dynamic water simulation model (DWSM) (in Chinese). *South-to-North Water Transfers Water Sci. Tech, 6*, 28-31.